Coffman et al., http://www.jcb.org/cgi/content/full/jcb.201305022/DC1

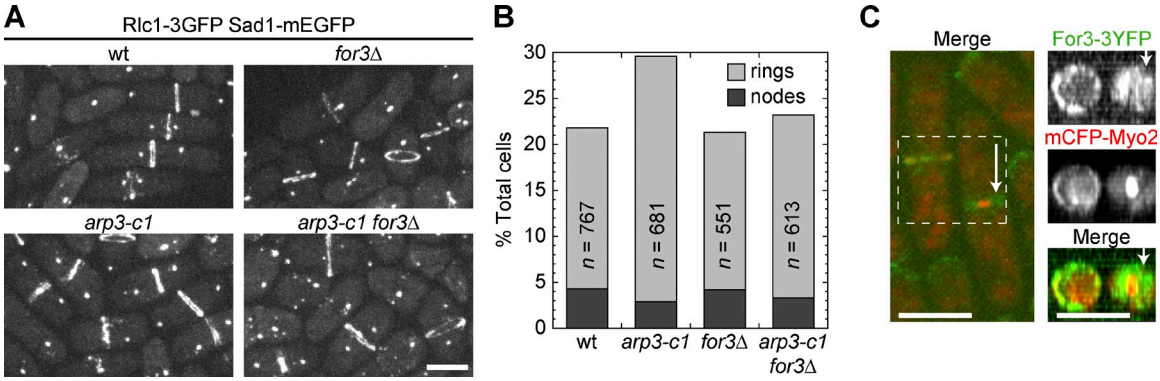

Figure S1. **Contractile ring formation and constriction in *arp3-c1* and *for3Δ* single and double mutants.** (A) Contractile ring formation and constriction in *arp3-c1* and *for3Δ* single and double mutants after 16 h at the restrictive temperature of 19°C. Cells were imaged at 19°C. Sad1 labels the SPBs and Rlc1 the rings. (B) Quantification of the cell populations as in A with contractile rings and cytokinesis nodes. (C) For3 and Myo2 localization in full size or constricting contractile rings. For3 colocalizes with Myo2 at the constricting ring but also localizes to the forming septum (arrows). Left, maximum intensity projection; right, 90° rotations of the boxed region. Bars, 5 µm.

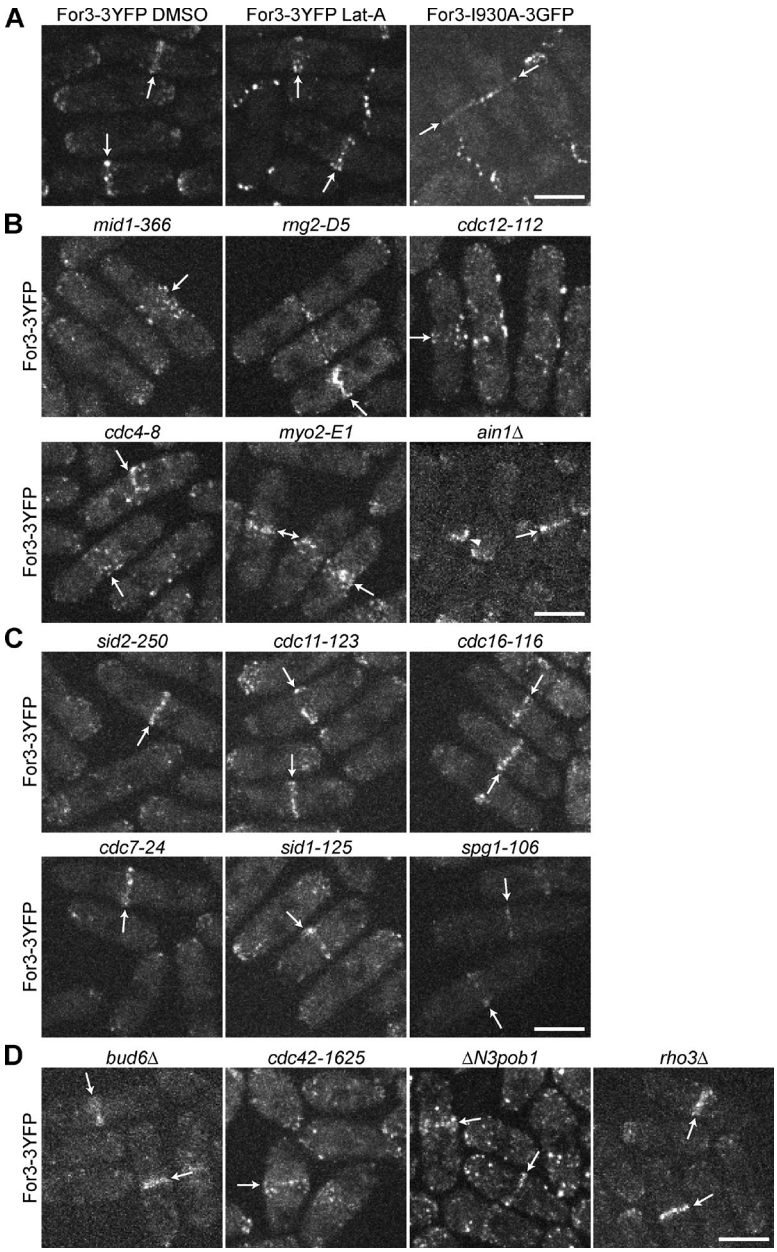

Figure S2. **For3 localization to the division site independent of cytokinesis and polarity mutants.** (A) Micrographs showing For3 localization to the division site (arrows) independently of filamentous actin or its own actin binding capacity. (B–D) Strains with ts alleles were imaged at 36°C after growing at 36°C for 4 h. (B) Micrographs showing For3 localization to the division site (arrows) in several cytokinesis mutants and to the clump (arrowhead) in *ain1Δ*. (C) Micrographs showing For3 localization to the division site (arrows) in septation initiation network mutants. (D) Micrographs showing For3 localization to the division site (arrows) in polarity mutants. Bars, 5 µm.

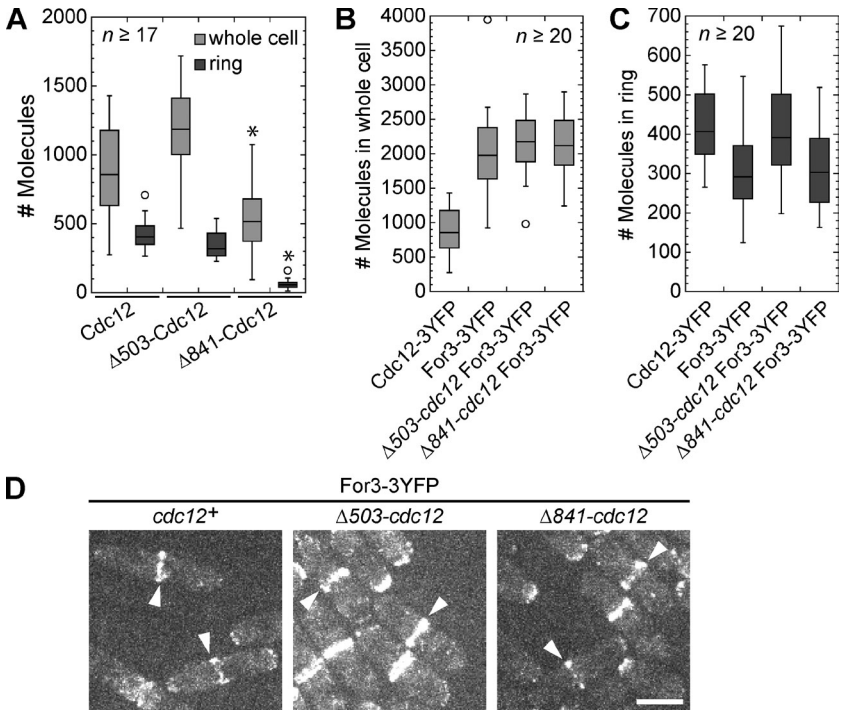

Figure S3. **Expression levels and localizations of Cdc12 truncations and For3.** (A) Box plots of 3YFP-tagged Cdc12 molecules in the whole cell (light gray) and in the contractile ring in anaphase B cells (dark gray) using full-length Cdc12-3YFP as a known standard (Wu and Pollard, 2005). *, $P < 0.005$ compared with molecules in the whole cell or the ring in wt, respectively. (B and C) Cdc12 data are repeated as a standard to count For3. (B) Box plots of For3 molecules in the whole cell during anaphase B in wt, *Δ503-cdc12*, and *Δ841-cdc12*. (C) Box plots of For3 molecules in the contractile ring of anaphase B cells in wt, *Δ503-cdc12*, and *Δ841-cdc12*. (D) Localization of For3-3YFP to the division site (arrowhead) in wt, *Δ503-cdc12*, and *Δ841-cdc12*. Bar, 5 μm.

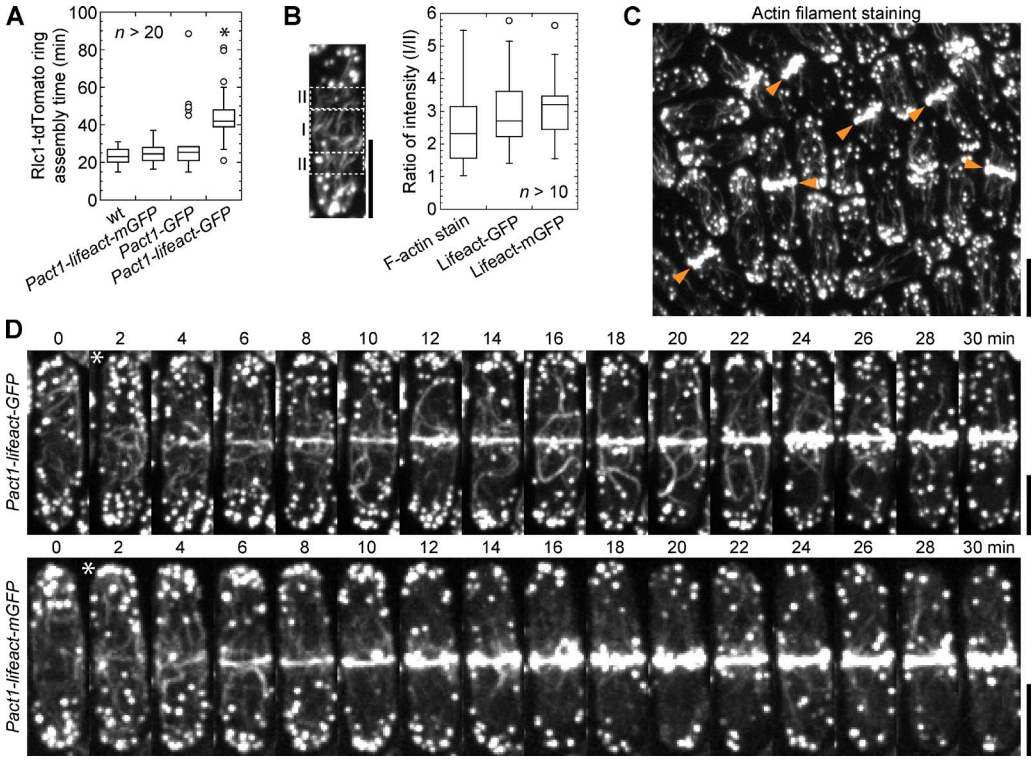

Figure S4. **Characterization of cells expressing Lifeact-mGFP and Lifeact-GFP.** (A) Box plots of timing of contractile ring assembly (from Rlc1 node appearance to a compact ring) in four strains at 23°C. *, P < 0.001 compared with wt. (B) Box plots of intensity of actin filaments in fixed and stained wt cells as in C and in live cells expressing Lifeact-GFP or Lifeact-mGFP. Ratio of integrated intensity of actin filaments at the broad band (I) compared with the area (II) just outside the broad band during the early stage of ring formation; regions of I and II (with the same areas) as pictured to the left. (C) Actin filament staining of wt cells. Cells with compact rings are marked by arrowheads. (D) Time courses of contractile ring assembly in cells expressing Lifeact-GFP (top) and Lifeact-mGFP (bottom) from the actin promoter. Micrographs at 2 min (marked with an asterisk) are representative of those cells measured in B. Bars, 5 µm.

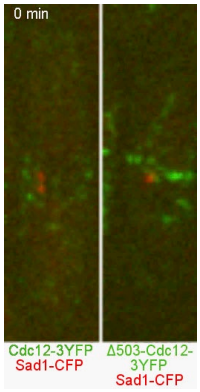

Video 1. **Contractile ring assembly from a band of Cdc12 nodes or node-like structures.** Contractile ring assembly from a band of Cdc12 nodes or node-like structures in wt (left) and *Δ503-cdc12* (right). The interval is 1 min in time-lapse confocal microscopy (UltraVIEW ERS; PerkinElmer). The intensity of Δ841-Cdc12-3YFP was lower and photobleached too rapidly to see ring formation clearly. This video corresponds to Fig. 3 B. Display rate is 8 frames per second (fps).

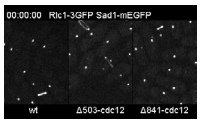

Video 2. **Contractile ring assembly from a broad band of Rlc1-3GFP nodes.** Contractile ring assembly from a broad band of Rlc1-3GFP nodes in wt (left), *Δ503-cdc12* (middle), and *Δ841-cdc12* (right). The SPB is also marked with Sad1-mEGFP. The interval is 30 s in time-lapse confocal microscopy (UltraVIEW ERS; PerkinElmer). This video corresponds to cells analyzed in Fig. 3 C. Display rate is 16 fps.

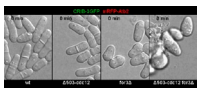

Video 3. **Time courses of CRIB-3GFP mRFP-Atb2.** Time courses of CRIB-3GFP mRFP-Atb2 in wt (left), *Δ503-cdc12* (middle left), *for3Δ* (middle right), and *Δ503-cdc12 for3Δ* (right). CRIB-3GFP is a marker for active Cdc42 and thus cell polarization. MTs are marked with mRFP-Atb2. The interval is 10 min in tetrad fluorescence microscopy (UltraVIEW Vox CSUX1 system; PerkinElmer). This video corresponds to Fig. 5 D. Display rate is 8 fps.

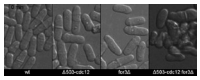

Video 4. **Contractile ring assembly and constriction.** Contractile ring assembly (from a broad band of Rlc1-tdTomato nodes) and constriction in wt (left), *Δ503-cdc12* (middle left), *for3Δ* (middle right), and *Δ503-cdc12 for3Δ* (right). The interval is 6 ± 2 min because of the time taken to autofocus at every third time point in tetrad fluorescence microscopy (UltraVIEW Vox CSUX1 system; PerkinElmer). This video corresponds to Fig. 5 (E and F). Display rate is 8 fps.

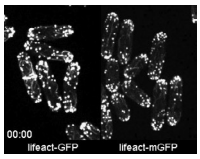

Video 5. **Visualization of Lifeact-GFP and Lifeact-mGFP during contractile ring assembly.** The interval is 1 min in time-lapse confocal microscopy (UltraVIEW Vox CSUX1 system; PerkinElmer). This video corresponds to Fig. S4 D. Display rate is 8 fps.

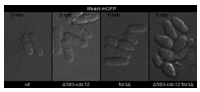

Video 6. **Visualization of Lifeact-mGFP during the cell cycle.** Visualization of Lifeact-mGFP during the cell cycle in wt (left), *Δ503-cdc12* (middle left), *for3Δ* (middle right), and *Δ503-cdc12 for3Δ* (right). The interval is 10 min in tetrad fluorescence microscopy (UltraVIEW Vox CSUX1 system; PerkinElmer). This video corresponds to Fig. 6 A. Display rate is 8 fps.

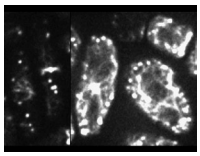

Video 7. **Visualization of Lifeact-mGFP in wt and *Δ503-cdc12 for3Δ* cells.** The interval is 5 s in tetrad fluorescence microscopy (UltraVIEW Vox CSUX1 system; PerkinElmer). Dividing cells in both wt (left) and double mutant (right) have a clear bias of movement toward the division site. This video corresponds to Fig. 6 C. Display rate is 8 fps.

Table S1. ***S. pombe* strains used in this study**

Strain name	Genotype	Figure/table and source/reference
JW1974	*cdc12-112 kanMX6-Pmyo2-YFP-myo2 sad1-mCFP-kanMX6 ade6-M210 leu1-32 ura4-D18*	Fig. 1 A
JW1404	*h⁺ cdc12-3YFP-kanMX6 ade6 leu1-32 ura4-D18*	Fig. 1 B; and Fig. S3, A–C; Coffman et al., 2009
JW1577	*h⁺ cdc12-112-3YFP-kanMX6 ade6-M210 leu1-32 ura4-D18*	Fig. 1 B
JW3136	*h⁻ cdc12-299-3YFP-kanMX6 ade6-M210 leu1-32 ura4-D18*	Fig. 1 B
JW1110	*h⁺ kanMX6-Pmyo2-mYFP-myo2 ade6-M210 leu1-32 ura4-D18*	Fig. 1 H; Wu and Pollard, 2005
JW1959	*h⁻ kanMX6-Pmyo2-mYFP-myo2 ade6-M216 leu1-32 ura4-D18*	Fig. 1 H; Laporte et al., 2011
JW1568	*h⁻ rlc1-3GFP-kanMX6 sad1-mEGFP-kanMX6 ade6-M210 leu1-32 ura4-D18*	Fig. 2, A and H; and Fig. S1, A and B; Wu et al., 2011
JW2211	*for3Δ::kanMX6 rlc1-3GFP-kanMX6 sad1-mEGFP-kanMX6 ade6 leu1-32 ura4-D18*	Fig. 2, A and H; and Fig. S1, A and B
JW1870	*sad1-CFP-kanMX6 for3-3YFP-kanMX6 ade6-M210 leu1-32 ura4-D18*	Fig. 2 B; and Fig. S3, B–D
JW5558	*Patb2-CFP-atb2 cdc15-140 for3-3YFP-kanMX6 ade6-M210 leu1-32 ura4-D18*	Fig. 2 C
JW5565	*Patb2-CFP-atb2 for3-3YFP-kanMX6 ade6-M210 leu1-32 ura4-D18*	Fig. 2 C
JW4991	*cdc15-mCherry-natMX6 cdc12-112 for3-3YFP-kanMX6 ade6-M210 leu1-32 ura4-D18*	Fig. 2, D and E
JW3151	*for3Δ::kanMX6 cdc12-112 rlc1-3GFP-kanMX6 sad1-mEGFP-kanMX6 ade6 leu1-32 ura4-D18*	Fig. 2, F–H
JW3159	*h⁻ cdc12-112 rlc1-3GFP-kanMX6 sad1-mEGFP-kanMX6 ade6 leu1-32 ura4-D18*	Fig. 2, F–H
JW2377	*h⁺ cdc12-112 ade6-M210 leu1-32 ura4-D18*	Fig. 2, I and J
JW3065	*h⁺ for3Δ::kanMX6 cdc12-112 ade6 leu1-32 ura4-D18*	Fig. 2, I and J
JW741	*h⁺ ade6-M216 leu1-32*	Fig. 2, I and J; Fig. 3, D and E; Fig. S4, B and C
JW1114	*h⁺ cdc12-3YFP-kanMX6 sad1-CFP-kanMX6 ade6 leu1-32 ura4-D18*	Figs. 3 B and 4 A; Wu et al., 2006; Coffman et al., 2009
JW2538	*sad1-mCFP-kanMX6 Pcdc12-Δ841-cdc12-3YFP-kanMX6 ade6 leu1-32 ura4-D18*	Figs. 3 B and 4 A
JW2615	*sad1-mCFP-hphMX6 Pcdc12-Δ503-cdc12-3YFP-kanMX6 ade6-M210 leu1-32 ura4-D18*	Figs. 3 B and 4 A
JW1576	*rlc1-3GFP-kanMX6 sad1-mEGFP-kanMX6 ade6 leu1-32*	Fig. 3 C
JW3253	*h⁻ ura4⁺-Pcdc12-Δ503-cdc12 rlc1-3GFP-kanMX6 sad1-mEGFP-kanMX6 ade6-M210 leu1-32 ura4-D18*	Fig. 3 C
JW3798	*ura4⁺-Pcdc12-Δ841-cdc12 rlc1-3GFP-kanMX6 sad1-mEGFP-kanMX6 ade6-M210 leu1-32 ura4-D18*	Fig. 3 C
JW1711	*h⁻ ura4⁺-Pcdc12-Δ503-cdc12 ade6-M210 leu1-32 ura4-D18*	Fig. 3, D and E; and Table 2
JW2443	*h⁻ ura4⁺-Pcdc12-Δ841-cdc12 ade6-M210 leu1-32 ura4-D18*	Fig. 3, D and E
JW2100	*h⁻ ura4⁺-Pcdc12-Δ503-cdc12-3YFP-hphMX6 ade6-M210 leu1-32 ura4-D18*	Fig. 4 B and Table 2
JW2257	*cdc15-140 ura4⁺-Pcdc12-Δ503-cdc12-3YFP-hphMX6 ade6-M210 leu1-32 ura4-D18*	Fig. 4 B
JW1665	*h⁻ for3Δ::kanMX6 rlc1-tdTomato-natMX6 ade6-M216 leu1-32 ura4-D18*	Fig. 5, A, B, E, and F
JW5124	*h⁺ rlc1-tdTomato-natMX6 ura4⁺-Pcdc12-Δ503-cdc12 ade6-M210 leu1-32 ura4-D18*	Fig. 5, A, B, E, and F
JW5281	*h⁺ for3Δ::kanMX6 Patb2-mRFP-atb2 P_{shk1}-CRIB-3GFP::ura4⁺ ade6 leu1-32 ura4-D18*	Fig. 5, A, C, and D
JW5283	*h⁻ ura4⁺-Pcdc12-Δ841-cdc12 Patb2-mRFP-atb2 P_{shk1}-CRIB-3GFP::ura4⁺ ade6 leu1-32 ura4-D18*	Fig. 5, A and C
JW5282-2	*h⁻ ura4⁺-Pcdc12-Δ503-cdc12 Patb2-mRFP-atb2 P_{shk1}-CRIB-3GFP::ura4⁺ ade6 leu1-32 ura4-D18*	Fig. 5 D
BFY9	*h⁻ for3Δ::kanMX6 ade6-M216 leu1-32 ura4-D18*	Fig. 5 G; F. Chang (Columbia University, New York, NY)
JW2196	*h⁺ Pcdc12-Δ503-cdc12-3YFP-kanMX6 ade6-M210 leu1-32 ura4-D18*	Fig. 5 G
JW3565	*h⁺ Pcdc12-Δ841-cdc12-3YFP-kanMX6 ade6 leu1-32 ura4-D18*	Fig. 5 G
JW5560	*h⁺ Patb2-mRFP-atb2 Pcdc12-Δ503-cdc12-3GFP-kanMX6 leu1-32 ura4-D18*	Fig. 5 H
JW5561	*h⁻ Patb2-mRFP-atb2 for3Δ::kanMX6 leu1-32 ura4-D18*	Fig. 5 H
JW5463	*h⁺ ura4⁺-Pcdc12-Δ503-cdc12 Pact1-lifeact-mGFP::leu1⁺ ade6-M210 leu1-32 ura4-D18*	Fig. 6 A
JW5481	*h⁻ for3Δ::kanMX6 Pact1-lifeact-mGFP::leu1⁺ ade6 leu1-32 ura4-D18*	Fig. 6 A
JW5462	*h⁺ ura4⁺-Pcdc12-Δ503-cdc12 rlc1-tdTomato-natMX6 Pact1-lifeact-mGFP::leu1⁺ ade6-M210 leu1-32 ura4-D18*	Fig. 6, B and C
JW5602	*h⁻ for3Δ::kanMX6 Pact1-lifeact-mGFP::leu1⁺ rlc1-tdTomato-natMX6 ade6 leu1-32 ura4-D18*	Fig. 6, B and C
JW3061	*arp3-c1 rlc1-3GFP-kanMX6 sad1-mEGFP-kanMX6 ade6 leu1-32 ura4-D18*	Fig. S1, A and B
JW3598	*for3Δ::kanMX6 arp3-c1 rlc1-3GFP-kanMX6 sad1-mEGFP-kanMX6 ade6 leu1-32 ura4-D18*	Fig. S1, A and B
JW2292	*kan^S Pmyo2-mCFP-myo2 for3-3YFP-kanMX6 ade6 leu1-32 ura4-D18*	Fig. S1 C

Table S1. ***S. pombe* strains used in this study** *(Continued)*

Strain name	Genotype	Figure/table and source/reference
JW1583-4	*h⁻ for3-3YFP-kanMX6 ade6-M210 leu1-32 ura4-D18*	Fig. S2 A
JW3137	*h⁻ for3-I930A-3GFP-ura4⁺ ade6 leu1-32 ura4-D18*	Fig. S2 A
JW2375	*rng2-D5 for3-3YFP-kanMX6 ade6 leu1-32 ura4-D18*	Fig. S2 B
JW2376	*cdc12-112 for3-3YFP-kanMX6 ade6-M210 leu1-32 ura4-D18*	Fig. S2 B
JW2380	*cdc4-8 for3-3YFP-kanMX6 ade6-M210 leu1-32 ura4-D18*	Fig. S2 B
JW2382	*myo2-E1 for3-3YFP-kanMX6 ade6 leu1-32 ura4-D18*	Fig. S2 B
JW2383	*mid1-366 for3-3YFP-kanMX6 ade6-M210 leu1-32 ura4-D18*	Fig. S2 B
JW4612	*ain1-Δ1::kanMX6 for3-3YFP-kanMX6 ade6-M210 leu1-32 ura4-D18*	Fig. S2 B
JW3459	*cdc16-116 for3-3YFP-kanMX6 ade6-M210 leu1-32 ura4-D18*	Fig. S2 C
JW3460	*cdc11-123 for3-3YFP-kanMX6 ade6-M210 leu1-32 ura4-D18*	Fig. S2 C
JW3461	*cdc7-24 for3-3YFP-kanMX6 ade6-M210 leu1-32 ura4-D18*	Fig. S2 C
JW3462	*sid1-125 for3-3YFP-kanMX6 ade6-M210 leu1-32 ura4-D18*	Fig. S2 C
JW3463	*spg1-106 for3-3YFP-kanMX6 ade6-M210 leu1-32 ura4-D18*	Fig. S2 C
JW3464	*sid2-250 for3-3YFP-kanMX6 ade6-M210 leu1-32 ura4-D18*	Fig. S2 C
JW3138	*rho3Δ::kanMX4 for3-3YFP-kanMX6 ade6 leu1-32 ura4-D18*	Fig. S2 D
JW3139	*for3-3YFP-kanMX6 bud6Δ::kanMX ade6 leu1-32 ura4-D18*	Fig. S2 D
JW3148	*HA-ΔN3pob1::ura4⁺ for3-3YFP-kanMX6 ade6 leu1-32 ura4-D18*	Fig. S2 D
JW3508	*h⁺ cdc42-1625(A158V)-kanMX for3-3YFP-kanMX6 ade6 leu1-32 ura4-D18*	Fig. S2 D
JW2167-5	*h⁻ Pcdc12-Δ841-cdc12-3YFP-kanMX6 ade6-M216 leu1-32 ura4-D18*	Fig. S3 A
JW2197	*h⁻ Pcdc12-Δ503-cdc12-3YFP-kanMX6 ade6-M210 leu1-32 ura4-D18*	Fig. S3 A
JW4296	*ura4⁺-Pcdc12-Δ503-cdc12 sad1-CFP-kanMX6 for3-3YFP-kanMX6 ade6-M210 leu1-32 ura4-D18*	Fig. S3, B–D
JW4297	*ura4⁺-Pcdc12-Δ841-cdc12 sad1-CFP-kanMX6 for3-3YFP-kanMX6 ade6-M210 leu1-32 ura4-D18*	Fig. S3, B–D
JW1341	*h⁻ rlc1-tdTomato-natMX6 ade6-M210 leu1-32 ura4-D18*	Fig. S4 A; Wu et al., 2011
JW5229	*Pact1-GFP::leu1⁺ rlc1-tdTomato-natMX6 ade6 leu1-32 ura4-D18*	Fig. S4 A
JW5188	*rlc1-tdTomato-natMX6 Pact1-lifeact-GFP::leu1⁺ ade6-M210 leu1-32 ura4-D18*	Fig. S4, A and B
JW5189	*rlc1-tdTomato-natMX6 Pact1-lifeact-mGFP::leu1⁺ ade6-M210 leu1-32 ura4-D18*	Fig. S4, A and B
MBY7200	*h⁻ Pact1-lifeact-GFP::leu1⁺ ade6-M216 ura4-D18*	Fig. S4 D; Huang et al., 2012
MBY7519	*h⁺ Pact1-lifeact-mGFP::leu1⁺ ade6-M210 leu1-32 ura4-D18*	Fig. S4 D; Huang et al., 2012
FC164	*h⁻ mid1-366*	Table 1; Chang et al., 1996
JW1312	*h⁻ for3Δ::kanMX6 41nmt1-GFP-CHD-leu1⁺ ade6 leu1-32 ura4-D18*	Table 1; Vavylonis et al., 2008
JW1313	*h⁺ for3Δ::kanMX6 41nmt1-GFP-CHD-leu1⁺ ade6 leu1-32 ura4-D18*	Table 1
JW2254	*h⁺ rlc1Δ::kanMX6 ade6-M210 leu1-32 ura4-D18*	Table 1
JW2738	*h⁺ cdc4-8 ade6-M210 leu1-32 ura4-D18*	Table 1
JW2740	*h⁺ cdc12-299 ade6-M210 leu1-32 ura4-D18*	Table 1
JW1049	*h⁺ for3Δ::kanMX6 ade6-M216 leu1-32 ura4-D18*	Tables 1 and 2
JW1743	*h⁺ cdc15-140 ade6-M210 leu1-32 ura4-D18*	Tables 1 and 2
YDM26	*h⁻ rng2-D5 ade6-M210 leu1-32 ura4-D18*	Tables 1 and 2; Eng et al., 1998
FC166	*h⁻ rng2-346*	Table 2; Chang et al., 1996
JW21	*h⁺ cdc4-8*	Table 2; Nurse et al., 1976; McCollum et al., 1995
JW768	*h⁻ rng3-65 ade6-216 leu1-32*	Table 2
JW901-3	*h⁻ mid1-366 ura4-D18*	Table 2
JW965	*h⁺ mid1-ΔF::ura4⁺ ade6 leu1-32 ura4-D18*	Table 2
JW1636	*h⁺ mid1-6 ade6-M210 leu1-32 ura4-D18*	Table 2
JW1657	*h⁻ ura4⁺-Pcdc12-Δ503-cdc12-3YFP-kanMX6 ade6-M210 leu1-32 ura4-D18*	Table 2
JW1825	*h⁺ blt1Δ::kanMX ade6-M216 leu1-32 ura4-D18*	Table 2; Ye et al., 2012
JW2104	*h⁺ ura4⁺-Pcdc12-Δ503-cdc12-3YFP-kanMX6 ade6-M210 leu1-32 ura4-D18*	Table 2
MLP9	*h⁻ rlc1Δ::kanMX6 ade6-M216 his7-366 leu1-32 ura4-D18*	Table 2; M. Lord (University of Vermont, Burlington, VT)
YDM74	*h⁻ myo2-E1 ade6-M216 his3-D1 leu1-32 ura4-D18*	Table 2; Balasubramanian et al., 1998
YSM616	*h⁺ for3-I930A-3GFP-ura4⁺ ade6-M216 leu1-32 ura4-D18*	Table 2; Martin and Chang, 2006
JW5125-3	*rlc1-tdTomato-natMX6 ura4⁺-Pcdc12-Δ841-cdc12 ade6-M210 leu1-32 ura4-D18*	This study

References

Balasubramanian, M.K., D. McCollum, L. Chang, K.C. Wong, N.I. Naqvi, X. He, S. Sazer, and K.L. Gould. 1998. Isolation and characterization of new fission yeast cytokinesis mutants. *Genetics*. 149:1265–1275.

Chang, F., A. Woollard, and P. Nurse. 1996. Isolation and characterization of fission yeast mutants defective in the assembly and placement of the contractile actin ring. *J. Cell Sci.* 109:131–142.

Coffman, V.C., A.H. Nile, I.-J. Lee, H. Liu, and J.-Q. Wu. 2009. Roles of formin nodes and myosin motor activity in Mid1p-dependent contractile-ring assembly during fission yeast cytokinesis. *Mol. Biol. Cell*. 20:5195–5210. http://dx.doi.org/10.1091/mbc.E09-05-0428

Eng, K., N.I. Naqvi, K.C.Y. Wong, and M.K. Balasubramanian. 1998. Rng2p, a protein required for cytokinesis in fission yeast, is a component of the actomyosin ring and the spindle pole body. *Curr. Biol.* 8:611–621. http://dx.doi.org/10.1016/S0960-9822(98)70248-9

Huang, J., Y. Huang, H. Yu, D. Subramanian, A. Padmanabhan, R. Thadani, Y. Tao, X. Tang, R. Wedlich-Soldner, and M.K. Balasubramanian. 2012. Nonmedially assembled F-actin cables incorporate into the actomyosin ring in fission yeast. *J. Cell Biol.* 199:831–847. http://dx.doi.org/10.1083/jcb.201209044

Laporte, D., V.C. Coffman, I.-J. Lee, and J.-Q. Wu. 2011. Assembly and architecture of precursor nodes during fission yeast cytokinesis. *J. Cell Biol.* 192:1005–1021. http://dx.doi.org/10.1083/jcb.201008171

Martin, S.G., and F. Chang. 2006. Dynamics of the formin for3p in actin cable assembly. *Curr. Biol.* 16:1161–1170. http://dx.doi.org/10.1016/j.cub.2006.04.040

McCollum, D., M.K. Balasubramanian, L.E. Pelcher, S.M. Hemmingsen, and K.L. Gould. 1995. *Schizosaccharomyces pombe cdc4*$^{+}$ gene encodes a novel EF-hand protein essential for cytokinesis. *J. Cell Biol.* 130:651–660. http://dx.doi.org/10.1083/jcb.130.3.651

Nurse, P., P. Thuriaux, and K. Nasmyth. 1976. Genetic control of the cell division cycle in the fission yeast *Schizosaccharomyces pombe. Mol. Gen. Genet.* 146:167–178. http://dx.doi.org/10.1007/BF00268085

Vavylonis, D., J.-Q. Wu, S. Hao, B. O'Shaughnessy, and T.D. Pollard. 2008. Assembly mechanism of the contractile ring for cytokinesis by fission yeast. *Science*. 319:97–100. http://dx.doi.org/10.1126/science.1151086

Wu, J.-Q., and T.D. Pollard. 2005. Counting cytokinesis proteins globally and locally in fission yeast. *Science*. 310:310–314. http://dx.doi.org/10.1126/science.1113230

Wu, J.-Q., V. Sirotkin, D.R. Kovar, M. Lord, C.C. Beltzner, J.R. Kuhn, and T.D. Pollard. 2006. Assembly of the cytokinetic contractile ring from a broad band of nodes in fission yeast. *J. Cell Biol.* 174:391–402. http://dx.doi.org/10.1083/jcb.200602032

Wu, P., R. Zhao, Y. Ye, and J.-Q. Wu. 2011. Roles of the DYRK kinase Pom2 in cytokinesis, mitochondrial morphology, and sporulation in fission yeast. *PLoS ONE*. 6:e28000. http://dx.doi.org/10.1371/journal.pone.0028000

Ye, Y., I.-J. Lee, K.W. Runge, and J.-Q. Wu. 2012. Roles of putative Rho-GEF Gef2 in division-site positioning and contractile-ring function in fission yeast cytokinesis. *Mol. Biol. Cell*. 23:1181–1195. http://dx.doi.org/10.1091/mbc.E11-09-0800